

Probing the Frequency Dispersion of the Magnetic Permeability of a Sample During Dynamic Interaction with a Magnetized Probe

© G.V. Dedkov

Kabardino-Balkarian State University,
360004 Nalchik, Kabardino-Balkaria, Russia
e-mail: gv_dedkov@mail.ru

Received February 5, 2022

Revised February 25, 2022

Accepted February 25, 2022

The forces acting on a magnetic particle during nonrelativistic motion parallel to the surface of a homogeneous medium with a frequency dispersion of magnetic permeability are considered. General expressions are obtained for the normal (attractive) and lateral (braking) forces acting on a small dipole particle and an extended probe. It is shown that for an arbitrary orientation of the vector of the dipole magnetic moment of the particle, along with the force of attraction and the stopping force, there also appears a velocity-dependent lateral force perpendicular to the velocity vector. The possibility of using the results to study the frequency-dependent magnetic permeability of nanostructured materials and films in the dynamic scanning mode of magnetic force microscopy with magnetic probes is discussed. Numerical estimates are given for the magnitude of the expected forces, friction coefficients, and changes in the quality factor of the MFM oscillators in the case of frequency dispersion of relaxation-type magnetic permeability.

Keywords: nanostructured magnetic materials, frequency dispersion of magnetic permeability, magnetic force microscopy.

DOI: 10.21883/TP.2022.05.53684.25-22

Introduction

Study of interaction of microwave range electromagnetic waves with magnetic materials is of great interest for development of technology of their manufacture and applications as concentrators or absorbers of microwave field [1–6]. In particular, electromagnetic wave equipment and devices operating at frequencies of 0.5–8 GHz are widely used in wireless communication, data transmission systems, local area networks, etc. Since many nanostructured materials have a complex dependence of magnetic permeability (MP) on frequency, there is a need to control the MP frequency dispersion to obtain high values of magnetic permeability, small losses or strong frequency dependence in a given range [7,8]. Standard methods to study MP frequency dispersion are the Nikolson–Ross–Weir method in a coaxial line or in free space, and the method for measuring MP of thin ferromagnetic films using a shorted cell [8]. However, these macroscopic methods prevent local probing of MP dispersion. Standard techniques of scanning magnetic force microscopy (SFM) [9,10] and magnetic-resonance force microscopy [11,12] make it possible to study the domain structure, spatial distribution of resonance properties and spectra of inherent magnetic vibrations of a sample. In this case, a magnetic probe serves either as a source of an external field acting on it or as a detector of magnetic torques. But in both cases quasistatic conservative magnetic interaction force of the probe and the sample is measured, for which the electrodynamic response contains almost no information on MP frequency dispersion of the surface material.

The aim of this paper is to discuss the possibility of local MFM probing of MP frequency dispersion in materials by measuring dissipative interaction force (friction force) between a magnetized probe and a sample in the non-contact interaction mode. The value of this force (viscous „friction“ coefficient) directly depends on the shape of the MP frequency dependence of the sample material. To this end, in Sections 1,2 general equations were produced for normal (conservative) and lateral (dissipative) forces of interaction with the surface of a point magnetic dipole particle and an extended probe in the form of a paraboloid of rotation (sphere) in non-relativistic motion parallel to the surface characterized by magnetic permeability $\mu(\omega)$. In Section 3 there are numerical calculations of the value of expected forces, friction and merit coefficients of an MFM oscillator in MP dispersion of relaxation type [5]. To record all values, unless otherwise specified, Gaussian system of units is used.

1. Interaction of a small dipole particle with surface

Let us first consider interaction of a small particle having constant dipole magnetic torque $\mathbf{m} = (m_x, m_y, m_z)$, with surface of homogeneous and isotropic medium characterized by magnetic permeability of general type $\mu(\omega) = \mu'(\omega) + i\mu''(\omega)$. Let us consider that a particle moves with constant speed \mathbf{V} in direction of an axis x of

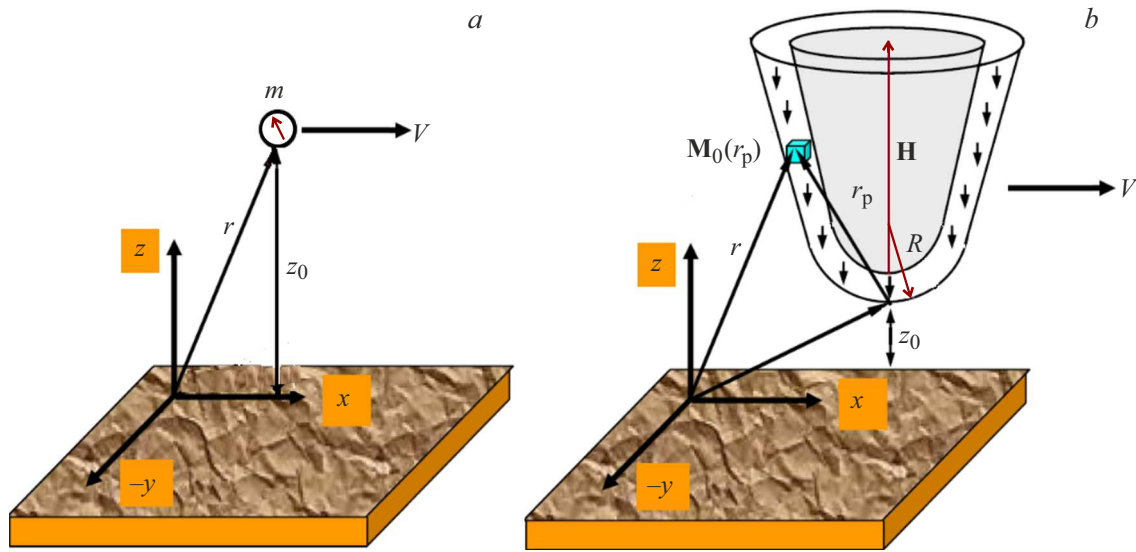


Figure 1. Scheme of interaction of a dipole magnetic particle (a) and an extended probe (b) with magnetic surface.

Cartesian coordinate system at distance z_0 from the surface (fig. 1, a).

In absence of external magnetic field, force acting on a particle shall be determined by classic electrodynamics equation [13]

$$\mathbf{F} = \text{grad}(\mathbf{m}\mathbf{H}), \quad (1)$$

where \mathbf{H} — vector of magnetic field induced by polarization current of the particle $\mathbf{j} = c \text{rot}\mathbf{M}$ (c — speed of light in vacuum, \mathbf{M} — polarization vector). For a point magnet dipole let us write \mathbf{M} in the form

$$\mathbf{M} = \mathbf{m}\delta(x - Vt)\delta(y)\delta(z - z_0). \quad (2)$$

Vector \mathbf{H} is found from ratio $\mathbf{H} = \text{rot}\mathbf{A}$, where \mathbf{A} — vector potential meeting equation

$$\Delta\mathbf{A} = -\frac{4\pi}{c}\mathbf{j}, \quad (3)$$

with the condition of Coulomb calibration $\text{div}\mathbf{A} = 0$. Equation (3) is decomposed into three Poisson equations for projections of vector potential A_x, A_y, A_z , similar to equation for scalar electric potential of the dipole in the configuration shown in fig. 1, a. The method to solve this and similar tasks is detailed in [14]. Let us break vector functions \mathbf{A} and \mathbf{M} into 3D Fourier integrals by components of a 2D wave vector $\mathbf{k} = (k_x, k_y)$ and by frequency ω :

$$\mathbf{A}(\mathbf{r}, t) = \int \frac{d^2k}{(2\pi)^2} \frac{d\omega}{2\pi} \mathbf{A}_{\mathbf{k}\omega}(z) \exp(i(k_x x + k_y y - \omega t)), \quad (4)$$

$$\mathbf{M}(\mathbf{r}, t) = \int \frac{d^2k}{(2\pi)^2} \frac{d\omega}{2\pi} \mathbf{M}_{\mathbf{k}\omega}(z) \exp(i(k_x x + k_y y - \omega t)), \quad (5)$$

where $\mathbf{r} = (\rho, z) = (x, y, z)$. Using (2), we get $\mathbf{M}_{\mathbf{k}\omega}$ using inverted Fourier transform

$$\begin{aligned} \mathbf{M}_{\mathbf{k}\omega}(z) &= \int dx dy dt \mathbf{M}(\mathbf{r}, t) \exp(i(k_x x + k_y y - \omega t)) \\ &= 2\pi \mathbf{m} \delta(\omega - k_x V) \delta(z - z_0). \end{aligned} \quad (6)$$

Similarly to (6) with account of link $\mathbf{j} = c \text{rot}\mathbf{M}$, for Fourier-transformat projections current density $\mathbf{j}_{\mathbf{k}\omega}(z)$ we will have

$$j_{\mathbf{k}\omega,x}(z) = 2\pi c \delta(\omega - k_x V) [ik_y m_z \delta(z - z_0) - m_y \delta'(z - z_0)], \quad (7)$$

$$j_{\mathbf{k}\omega,y}(z) = 2\pi c \delta(\omega - k_x V) [m_x \delta'(z - z_0) - ik_x m_z \delta(z - z_0)], \quad (8)$$

$$j_{\mathbf{k}\omega,z}(z) = 2\pi c \delta(\omega - k_x V) [ik_x m_y \delta(z - z_0) - ik_y m_x \delta(z - z_0)]. \quad (9)$$

Going in (3) to Fourier components, we will get the system of equations

$$(i = x, y, z, \quad k = \sqrt{k_x^2 + k_y^2}),$$

$$\left(\frac{d^2}{dz^2} - k^2\right) A_{\mathbf{k}\omega,i}(z) = -\frac{4\pi}{c} j_{\mathbf{k}\omega,i}(z). \quad (10)$$

It is convenient to find solution to equations (10) by parts, considering separately the cases with different orientation of dipole torque vector: $\mathbf{m} = (0, 0, m_z)$, $\mathbf{m} = (m_x, 0, 0)$ and $\mathbf{m} = (0, m_y, 0)$, and then summing the produced solutions. In case $\mathbf{m} = (0, 0, m_z)$, for example, suggesting $A_{\mathbf{k}\omega,z}(z) = 0$, equations (10) are reduced to the system of two equations

$$\left(\frac{d^2}{dz^2} - k^2\right) A_{\mathbf{k}\omega,x}(z) = -i8\pi^2 k_y m_z \delta(\omega - k_x V) \delta(z - z_0), \quad (11)$$

$$\left(\frac{d^2}{dz^2} - k^2\right)A_{\mathbf{k}\omega,y}(z) = i8\pi^2 k_x m_z \delta(\omega - k_x V) \delta(z - z_0). \quad (12)$$

The general solution to equations (11), (12) in areas $z > 0$ and $z \leq 0$ include four integration constants. One of the terms to determine such constants is calibration ratio $\text{div } \mathbf{A} = 0$, and three other proceed from terms of continuity of tangential projections of magnetic field H_x, H_y and normal projection of magnetic induction B_z at boundary $z = 0$. The procedure to solve equations (11), (12) is described in Annex. As a result, the following equations are produced for Fourier components of vector potential in vacuum area $z > 0$, necessary to calculate force (1):

$$A_{\mathbf{k}\omega,x}(z) = i \frac{(2\pi)^2}{k} k_y m_z \left[\frac{\mu - 1}{\mu + 1} \exp(-k(z + z_0)) + \exp(-k|z - z_0|) \right] \delta(\omega - k_x V), \quad (13)$$

$$A_{\mathbf{k}\omega,y}(z) = -i \frac{(2\pi)^2}{k} k_x m_z \left[\frac{\mu - 1}{\mu + 1} \exp(-k(z + z_0)) + \exp(-k|z - z_0|) \right] \delta(\omega - k_x V). \quad (14)$$

In formulae (13) and (14) the first terms in brackets comply with induced field of the surface, and second ones — the own field of the particle in vacuum. Similarly solutions to equations (10) are found for other projections of dipole torque (see Annex). In the general case $\mathbf{m} = (m_x, m_y, m_z)$, after summing the corresponding induced Fourier components of the vector potential described by equations (13), (14) and (P8)–(P11), we will have

$$A_{\mathbf{k}\omega,x}(z) = \frac{(2\pi)^2}{k} \left(\frac{\mu - 1}{\mu + 1} \right) (im_z k_y - m_y k) \times \exp(-k(z + z_0)) \delta(\omega - k_x V), \quad (15)$$

$$A_{\mathbf{k}\omega,y}(z) = \frac{(2\pi)^2}{k} \left(\frac{\mu - 1}{\mu + 1} \right) (-im_z k_x + m_x k) \times \exp(-k(z + z_0)) \delta(\omega - k_x V), \quad (16)$$

$$A_{\mathbf{k}\omega,z}(z) = \frac{(2\pi)^2}{k} \left(\frac{\mu - 1}{\mu + 1} \right) (im_x k_y - im_y k_x) \times \exp(-k(z + z_0)) \delta(\omega - k_x V). \quad (17)$$

Function $\Delta(\omega) = (\mu(\omega) - 1)/(\mu(\omega) + 1)$ in (15)–(17) is similar to the surface dielectric response function in interaction with an electric dipole \mathbf{d} (as well as with charges and particles with other multipole torques) with replacement of $\mu(\omega) \rightarrow \varepsilon(\omega)$ [14]. Substituting (15)–(17) into (4), we obtain value of the magnetic field, $\mathbf{H} = \text{rot } \mathbf{A}$. In this case, in integral equations for vector projections \mathbf{H} there are derivatives on the coordinates x, y, z , effect of which is reduced to multiplication of the corresponding Fourier components by ik_x, ik_y and $-k$. Resulting equations for

Fourier-transformant projections of induced magnetic field have the form

$$H_{\mathbf{k}\omega,x}(z) = kA_{\mathbf{k}\omega,y}(z) + ik_y A_{\mathbf{k}\omega,z}(z) = A(m_x k_x^2 + m_y k_x k_y - im_z k_x k), \quad (18)$$

$$H_{\mathbf{k}\omega,y}(z) = -ik_x A_{\mathbf{k}\omega,z}(z) - kA_{\mathbf{k}\omega,x}(z) = A(m_y k_y^2 + m_x k_x k_y - im_z k_y k), \quad (19)$$

$$H_{\mathbf{k}\omega,z}(z) = ik_x A_{\mathbf{k}\omega,y}(z) - ik_y A_{\mathbf{k}\omega,x}(z) = A(m_z k^2 + im_x k_x k + im_y k_y k), \quad (20)$$

where

$$A = \frac{(2\pi)^2}{k} \Delta(\omega) \exp(-k(z + z_0)) \delta(\omega - k_x V). \quad (21)$$

Substituting (18)–(20) into Fourier expansion for \mathbf{H} and then into (1), after some simple transformations formula (1) takes the form

$$\mathbf{F} = \frac{1}{2\pi} \text{grad} \int d^2 k k^{-1} (m_x^2 k_x^2 + m_y^2 k_y^2 + m_z^2 k^2 + 2m_x m_y k_x k_y) \times \Delta(k_x V) \exp(-k(z + z_0)) \exp(ik_x(x - Vt) + ik_y y), \\ x = Vt, \quad y = 0, \quad z = z_0. \quad (22)$$

Note that to find different projections of vector \mathbf{F} in (22), first differentiation is carried out by coordinates x, y, z , and then coordinates of particle $x = Vt, y = 0, z = z_0$ are substituted. As a result, given analytical properties of function $\Delta(\omega)$ (parity of the real part and non-parity of the imaginary part), from (22) it follows that

$$F_z = -\frac{1}{2\pi} \int_{-\infty}^{+\infty} dk_x \int_{-\infty}^{+\infty} dk_y \Delta'(k_x V) (m_x^2 k_x^2 + m_y^2 k_y^2 + m_z^2 k^2) \times \exp(-2kz_0), \quad (23)$$

$$F_x = -\frac{1}{2\pi} \int_{-\infty}^{+\infty} dk_x \int_{-\infty}^{+\infty} dk_y \Delta''(k_x V) k_x k^{-1} \times (m_x^2 k_x^2 + m_y^2 k_y^2 + m_z^2 k^2) \exp(-2kz_0), \quad (24)$$

$$F_y = -\frac{m_x m_y}{\pi} \int_{-\infty}^{+\infty} dk_x \int_{-\infty}^{+\infty} dk_y \Delta''(k_x V) k_x k_y^2 k^{-1} \exp(-2kz_0). \quad (25)$$

Formulae (23) and (24) fully coincide with similar equations for interaction force of a moving electric dipole \mathbf{d} with dielectric surface (when substituting $\mathbf{m} \rightarrow \mathbf{d}$, $\mu(\omega) \rightarrow \varepsilon(\omega)$). Besides, (23) describes force of dipole attraction to surface, and (24) — dissipative (braking) force. In linear decomposition by speed (24) reduces to friction force of viscous nature, proportionate to speed $F_x \propto V$. Further we will always call dissipative force F_x the friction

force. The force F_y component has no electric analog and is also proportional to speed in linear decomposition by V , but for its existence the difference from zero in projections of m_x and m_y of magnetic torque is necessary. As a result, as it follows from (23)–(25), directions of all three components of the magnetic force are opposite to directions of the coordinate axes in fig. 1 (with positive values of the integrals).

2. Interaction of extended probe with surface

Point dipole approximation loses force at particle sizes comparable to the size of distance from the surface. However, the theory developed in Section 1, is easy to generalize by dividing the volume of a uniformly magnetized particle into elementary components ΔV_n and using superposition principle to find the resultant force (fig. 1, *b*). With this modification, instead of equation (2), we have

$$\mathbf{M}(x, y, z, t) = \sum_n \mathbf{m}_n \delta(x - x_n - Vt) \delta(y - y_n) \delta(z - z_n), \quad (26)$$

where \mathbf{m}_n — magnetic torque, and x_n, y_n, z_n — coordinates of elementary volume ΔV_n . Given that (26), for Fourier component of magnetic polarization vector we will get (cp. with (6))

$$\mathbf{M}_{\mathbf{k}\omega}(z) = 2\pi\delta(\omega - k_x V) \sum_n \mathbf{m}_n \exp(-i\mathbf{k}\boldsymbol{\rho}_n) \delta(z - z_n), \quad (27)$$

where $\boldsymbol{\rho} = (x_n, y_n)$ — 2D vector of coordinates of volume ΔV_n in plane (x, y) . Further procedure to calculate induced magnetic field fully repeats Section 1. In particular, formula (18) for Fourier transformant $H_{\mathbf{k}\omega, x}(z)$ takes the form of

$$\begin{aligned} H_{\mathbf{k}\omega, x}(z) &= \frac{(2\pi)^2}{k} \Delta(\omega) \exp(-k(z + z_0)) \delta(\omega - k_x V) \\ &\times \sum_n (m_{x,n} k_x^2 + m_{y,n} k_x k_y - i m_{z,n} k_x k) \\ &\times \exp(-k(z + z_0)) \exp(-i\mathbf{k}\boldsymbol{\rho}_n) \end{aligned} \quad (28)$$

and similarly for other components (compare to (18)–(20)). In (28) designations of projections $m_{j,n}$ of vector \mathbf{m}_n are used at $j = x, y, z$. With account of (28) and similar equations for other Fourier components of magnetic field, formulae for projections of force, similar to (23)–(25), take the form of

$$\begin{aligned} F_x &= -\frac{1}{2\pi} \sum_n \sum_{n'} \int_{-\infty}^{+\infty} dk_x \int_{-\infty}^{+\infty} dk_y \Delta'(k_x V) \\ &\times \exp(-k(z_n + z_{n'})) \exp(-i\mathbf{k}(\boldsymbol{\rho}_n - \boldsymbol{\rho}_{n'})) \\ &\times (m_{x,n} m_{x,n'} k_x^2 + m_{y,n} m_{y,n'} k_y^2 + m_{z,n} m_{z,n'} k^2), \end{aligned} \quad (29)$$

$$\begin{aligned} F_x &= -\frac{1}{2\pi} \sum_n \sum_{n'} \int_{-\infty}^{+\infty} dk_x \int_{-\infty}^{+\infty} dk_y \Delta''(k_x V) k_x k^{-1} \\ &\times \exp(-k(z_n + z_{n'})) \exp(-i\mathbf{k}(\boldsymbol{\rho}_n - \boldsymbol{\rho}_{n'})) \\ &\times (m_{x,n} m_{x,n'} k_x^2 + m_{y,n} m_{y,n'} k_y^2 + m_{z,n} m_{z,n'} k^2), \end{aligned} \quad (30)$$

$$\begin{aligned} F_y &= -\frac{1}{\pi} \sum_n \sum_{n'} m_{x,n} m_{y,n'} \int_{-\infty}^{+\infty} dk_x \int_{-\infty}^{+\infty} dk_y \Delta''(k_x V) k_x k_y^2 k^{-1} \\ &\times \exp(-k(z_n + z_{n'})) \exp(-i\mathbf{k}(\boldsymbol{\rho}_n - \boldsymbol{\rho}_{n'})). \end{aligned} \quad (31)$$

In practically critical cases for probes having cylindrical symmetry, equations (29)–(31) may be additionally simplified. Let us consider the two most critical ones.

2.1. Probe in the form of paraboloid of rotation

Let us consider homogeneously magnetized probe with vertical direction of magnetization vector in the entire volume ($\mathbf{M}_0 \parallel z$), having the form of paraboloid of rotation: $z = z_0 + \rho^2/2R$, $z_0 \leq z < z_0 + H$, $H \gg R$ (fig. 1, *b*). Writing \mathbf{m}_n and $\mathbf{m}_{n'}$ in the form of

$$\mathbf{m}_n = \mathbf{M}_0 \Delta V_n = \mathbf{M}_0 \rho d\rho dz d\phi,$$

$$\mathbf{m}_{n'} = \mathbf{M}_0 \Delta V_{n'} = \mathbf{M}_0 \rho' d\rho' dz' d\phi'$$

and changing in (30) from summation by n and n' to integrals by probe volume, after integration by angles ϕ, ϕ' and by coordinates ρ, ρ' , we will get

$$\begin{aligned} F_x &= -2\pi M_0^2 \int dk_x dk_y k^{-1} k_x \Delta''(k_x V) \int_{z_0}^{H+z_0} dz \sqrt{2R(z-z_0)} \\ &\times J_1(k\sqrt{2R(z-z_0)}) \exp(-kz) \int_{z_0}^{H+z_0} dz' \sqrt{2R(z'-z_0)} \\ &\times J_1(k\sqrt{2R(z'-z_0)}) \exp(-kz'). \end{aligned} \quad (32)$$

When formula (32) is made, determination of Bessel function is taken into account,

$$J_0(x) = \frac{1}{2\pi} \int_0^{2\pi} \exp(\pm i x \cos y) dy \quad (33)$$

as well as integral ratio $\int dx x J_0(x) = x J_1(x)$ [15]. Just similarly (29) is transformed as well. Lateral force (31) for such orientation of magnetization vector is unavailable. Since internal integrals in (32) are identical, after replacement of variables $u = k\sqrt{2R(z-z_0)}$ and $u' = k\sqrt{2R(z'-z_0)}$, taking into account analytical properties of function $\Delta(k_x V)$,

formula (32) takes the form of

$$F_x = -2\pi R^{-2} M_0^2 \int_{-\infty}^{+\infty} dk_x \int_{-\infty}^{+\infty} dk_y k_x k^{-7} \Delta''(k_x V) \times \exp(-2kz_0) f_1(2kR, \sqrt{H/2R})^2, \tag{34}$$

where function $f_1(x, y)$ is determined by equation

$$f_1(x, y) = \int_0^{xy} du u^2 J_1(u) \exp(-u^2/x). \tag{35}$$

Similarly for F_z we will have

$$F_z = -2\pi R^{-2} M_0^2 \int_{-\infty}^{+\infty} dk_x \int_{-\infty}^{+\infty} dk_y k^{-6} \Delta'(k_x V) \times \exp(-2kz_0) f_1(2kR, \sqrt{H/2R})^2. \tag{36}$$

For practical use of these common results it is necessary to use specific equations for magnetic response function $\Delta(\omega)$. Standard approximation for magnetic permeability $\mu(\omega)$ is [5]

$$\mu(\omega) = 1 + \frac{\mu_s - 1}{1 - i\omega\tau - (\omega/\omega_0)^2}, \tag{37}$$

where τ and ω_0 — time of relaxation and frequency of ferromagnetic resonance, $\mu_s = \mu(0)$. Typical values ω_0 make $10^9 - 10^{10} \text{ s}^{-1}$. At frequencies $\omega \ll \omega_0$ a resonant member in denominator (37) may be omitted. Then, taking into account (37), equation for $\Delta(\omega) = (\mu(\omega) - 1)/(\mu(\omega) + 1)$ takes the form of

$$\Delta(\omega) = \frac{\mu_s^2 - 1}{(\mu_s + 1)^2 + 4\omega^2\tau^2} + i \frac{2\omega\tau(\mu_s - 1)}{(\mu_s + 1)^2 + 4\omega^2\tau^2}. \tag{38}$$

Substituting (38) in (34), (36), after transfer to polar coordinates for wave vector (k_x, k_y) and integration by angles with account of tabular integral

$$\int_0^{2\pi} d\phi \cos^2 \phi / (1 + x^2 \cos^2 \phi) = 2\pi x^{-2} (1 - (1 + x^2)^{-1/2}),$$

we will get

$$F_x = -32\pi^2 \frac{(\mu_s - 1)}{(\mu_s + 1)} M_0^2 R^2 \frac{1}{a} \int_0^\infty dt t^{-6} \times e^{-pt} (1 - (1 + a^2 t^2)^{-1/2}) f_1(t, q)^2, \tag{39}$$

$$F_z = -64\pi^2 \frac{(\mu_s - 1)}{(\mu_s + 1)} M_0^2 R^2 \int_0^\infty dt t^{-5} \times e^{-pt} (1 + a^2 t^2)^{-1/2} f_1(t, q)^2, \tag{40}$$

where $a = 2V\tau/R(\mu_s + 1)$, $p = z_0/R$, $q = \sqrt{2H/R}$. At $a \ll 1$ equations (39) and (40) reduce to

$$F_x = -32\pi^2 \frac{(\mu_s - 1)}{(\mu_s + 1)^2} M_0^2 R V \tau \int_0^\infty dt t^{-4} e^{-pt} f_1(t, q)^2, \tag{41}$$

$$F_z = -64\pi^2 \frac{(\mu_s - 1)}{(\mu_s + 1)} M_s^2 R^2 \left[\int_0^\infty dt t^{-5} e^{-pt} f_1(t, q)^2 - \frac{a^2}{2} \int_0^\infty dt t^{-3} e^{-pt} f_1(t, q)^2 \right]. \tag{42}$$

At $a \ll 1$, it is evident, the second term in (42) represents only a small correction proportionate to squared speed. If a parabolic probe is not continuous but is coated by a magnetized layer of h thickness, and parameters R and H characterize the coated probe, then formulae (38)–(42) may easily be modified by subtracting similar equations with modified parameters $R \rightarrow R-h$, $z_0 \rightarrow z_0 + h$ from the right-hand parts.

2.2. Probe in the form of sphere

For a spherical probe with radius R and surface equation $(z - R - z_0)^2 + \rho^2 = R^2$ whose center is at distance $R + z_0$ from the sample surface, as a result of calculations similar to the previous case we will get

$$F_x = -16\pi^2 \frac{(\mu_s - 1)}{(\mu_s + 1)} M_s^2 R^2 a^{-1} \int_0^\infty dt (1 - (1 + a^2 t^2)^{-1/2}) \times \exp(-2t(1 + p)) f_2(t)^2, \tag{43}$$

$$F_z = -16\pi^2 \frac{(\mu_s - 1)}{(\mu_s + 1)} M_s^2 R^2 \int_0^\infty dt t (1 + a^2 t^2)^{-1/2} \times \exp(-2t(1 + p)) f_2(t)^2, \tag{44}$$

where still $p = z_0/R$, $a = 2V\tau/R(\mu_s + 1)$ and

$$f_2(x) = \int_0^1 dt t J_1(xt) \sinh(x\sqrt{1-t^2}). \tag{45}$$

At $a \ll 1$ respectively from (43), (44) it follows that

$$F_x = -16\pi^2 \frac{(\mu_s - 1)}{(\mu_s + 1)^2} M_s^2 R V \tau \int_0^\infty dt t^2 \exp(-2t(1 + p)) f_2(t)^2, \tag{46}$$

$$F_z = -16\pi^2 \frac{(\mu_s - 1)}{(\mu_s + 1)^2} M_s^2 R^2 \left[\int_0^\infty dt t \exp(-2t(1 + p)) f_2(t)^2 - \frac{a^2}{2} \int_0^\infty dt t^3 \exp(-2t(1 + p)) f_2(t)^2 \right]. \tag{47}$$

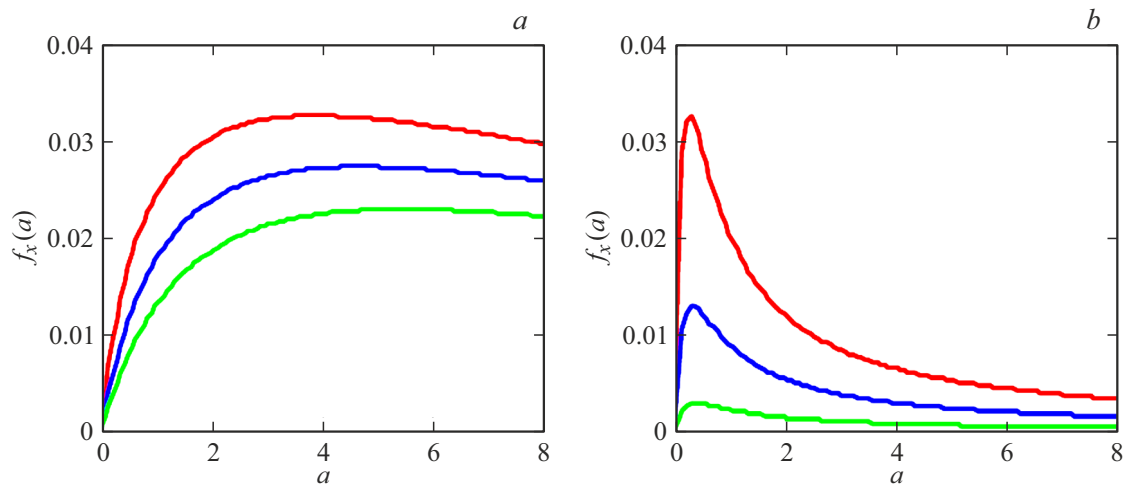


Figure 2. Dependence of reduced friction force on parameter $a = 2V\tau/(\mu_s + 1)R$ in case of a parabolic (a) and a spherical (b) probes. Sequence of curves from top to bottom complies with reduced distances $p = z_0/R = 0.1, 0.5, 1$ in case of (a) and $p = 0.1, 0.2, 0.4$ in case of (b). $q = 5$ in case of (a).

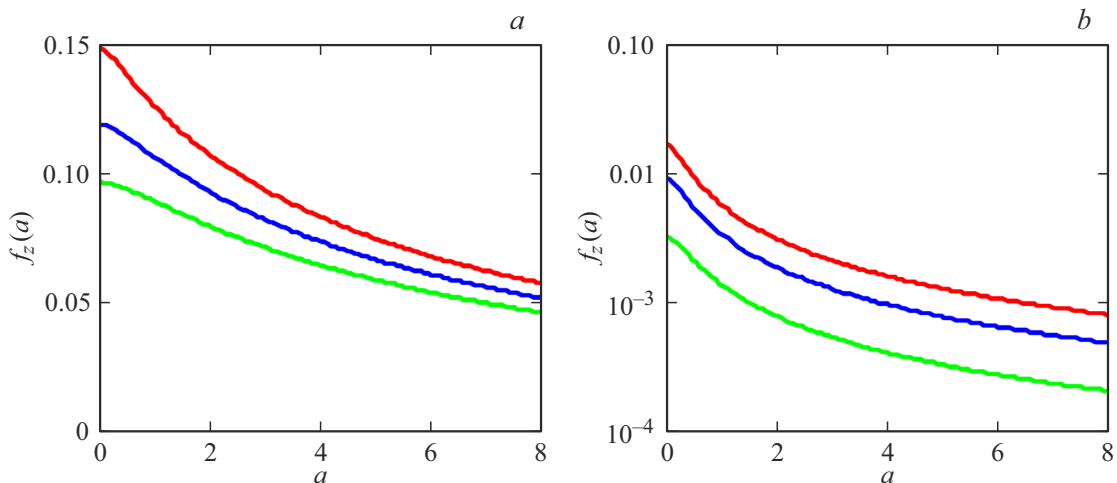


Figure 3. Reduced gravity force of a parabolic (a) and a spherical (b) probes to surface. Parameters are same as in fig. 2.

For a sphere coated by a magnetic layer with thickness h , subtract from right-hand parts (43) and (44) similar equations taken at $R \rightarrow R-h, z_0 \rightarrow z_0 + h$. For magnetic permeability of general type (37), common equations (34), (36) remain in force.

3. Numerical results and discussion

Let us first briefly consider influence of probe motion at value of forces F_x, F_z near resonance $\omega = \omega_0$ in dependence of MP (37). In accordance with (34) and (36), resonance may manifest itself, if $kV = \omega_0$. Value of wave vector k takes characteristic values $k = 1/2z_0$, therefore the corresponding speed of the probe will make $V_{res} \approx 2\omega_0 z_0$. Then at typical distance of the probe from the surface of 10 nm and frequency of ferromagnetic resonance $10^9 - 10^{11} \text{ s}^{-1}$ we will get speed estimate $V_{res} = 20 - 10^3 \text{ m/s}$. At the

same time, even at amplitude of vibrations $A = 1 \mu\text{m}$, quite significant for dynamic MFM mode, and typical frequency of mechanical oscillations $f = 300 \text{ kHz}$, the value of maximum speed of the probe is much smaller: $V_{max} = 2\pi f A \approx 1 \text{ m/s} \ll V_{res}$. Therefore, for MFM the case of MP relaxation dependence of type (38) is more realistic, when formulae (39)–(47) are fair. Such type of dispersion, for example, have ferrites $\text{Zn}_{1-x}\text{Ni}_x\text{Fe}_2\text{O}_4$ [16]. After normalization to value $F_0 = 32\pi^2 \frac{\mu_s - 1}{\mu_s + 1} M_0^2 R^2$ dependences $f_x = F_x/F_0$ and $f_z = F_z/F_0$ will be the functions of parameters p, q, a in case of a parabolic probe and parameters p, a in case of a spherical one. Let us note that at $\mu_s \gg 1, F = 10 \text{ nm}$ and $M_0 = 1740 \text{ G}$ (iron saturation magnetization [17]) value F_0 will be 9.13 nN.

Fig. 2,3 compare dependences f_x, f_z on parameter $a = 2V\tau/(\mu_s + 1)R$ at several values of reduced distance $p = z_0/R$ for a parabolic (fig. 2, a, 3, a) and spherical

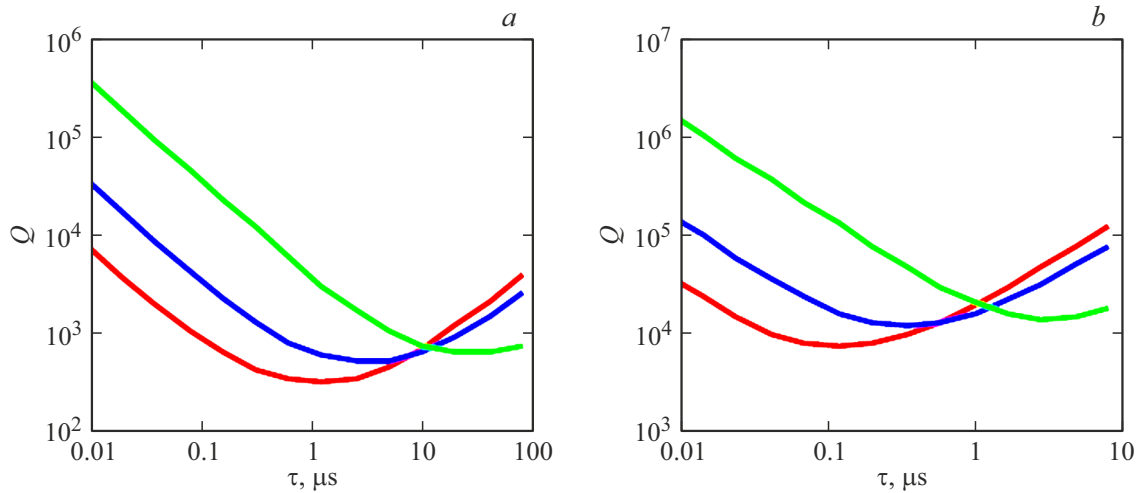


Figure 4. Dependence of MFM oscillator merit in case of a parabolic (*a*) and spherical (*b*) probes on relaxation time of sample magnetization. Sequence of curves from top to bottom complies with values of static magnetic permeability $\mu_s = 3, 10, 100$. In case (*a*) values $p = z_0/R = 0.5, q = 5$ are adopted; in case (*b*) $p = z_0/R = 0.2$.

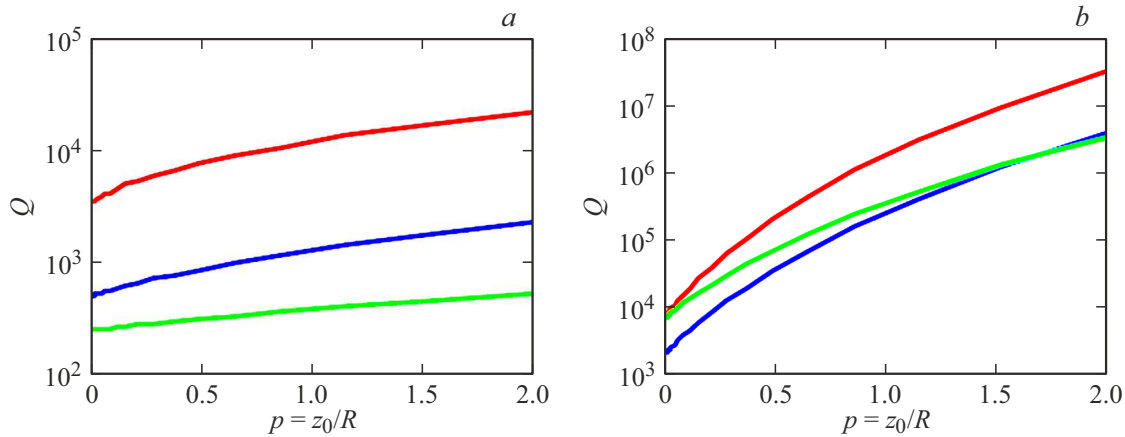


Figure 5. Dependence of MFM oscillator merit on reduced apex distance of a parabolic (*a*) and spherical (*b*) probes on surface. Sequence of curves from top to bottom complies with relaxation time of magnetization 0.01, 0.1 and 1 μs . In both cases $\mu_s = 3$ and $q = 5$ in case (*a*).

(fig. 2, *b*, 3, *b*) probes. Availability of extremum in dependences of friction force f_s on a (fig. 2) further leads to the non-monotone dependences of MFM oscillator merit Q , which is directly measured in the experiments. At $a \ll 1$ we can use standard definition of merit $Q = 2\pi f/\gamma$, where $\gamma = F_x/m_{\text{eff}}V$, m_{eff} — effective mass of the oscillator, and the friction force is defined by formulae (41) and (46). For a rectangular cantilever with a magnetic probe at the end, the value m_{eff} and inherent resonant frequency of the first harmonic of oscillations are $m_{\text{eff}} \approx 0.24lwh\rho$ and $f = (3.516/2\pi)h/l^2\sqrt{E/12\rho}$ [9], where l, w, h — length, width and thickness of rectangular beam, and ρ and E — density and Young’s modulus of material. Therefore, taking into account (41), for a cantilever with a parabolic probe at the end we will get

$$Q = 0.77 \cdot 10^{-3} \frac{h}{l} \frac{w}{R} \frac{(\mu_s + 1)^2 \sqrt{E\rho}}{(\mu_s - 1) M_0^2 \tau} \frac{h}{\varphi_1(p, q)}, \quad (48)$$

where function $\varphi_1(p, q) = F_x/F_0$ complies with an integral multiplier in (41). In all calculations we further use the following values of silicon cantilever parameters: $l = 100 \mu\text{m}$, $w = 20 \mu\text{m}$, $h = 5 \mu\text{m}$, $E = 150 \text{ GPa}$ and $\rho = 2.3 \text{ g/cm}^3$, $M_0 = 1740 \text{ G}$. As it follows from (48), merit Q monotonously decreases as relaxation time τ increases. For a spherical probe the numerical coefficient in (48) should be doubled, and instead of $\varphi_1(p, q)$ substitute a similar integral multiplier from (46).

As parameter a increases, friction forces (39) and (43) non-linearly depend on probe speed, therefore, to define merit, we use ratio $Q = E_0/\Delta E$, where $E_0 = 2\pi^2 f^2 A^2 m_{\text{eff}}$ — energy of oscillator at harmonic oscillations with amplitude A (in calculations we will further use value $A = 50 \text{ nm}$) and frequency f , and $\Delta E = \int_0^{1/f} F_x V dt$ — energy of dissipation for the period. In case of a parabolic

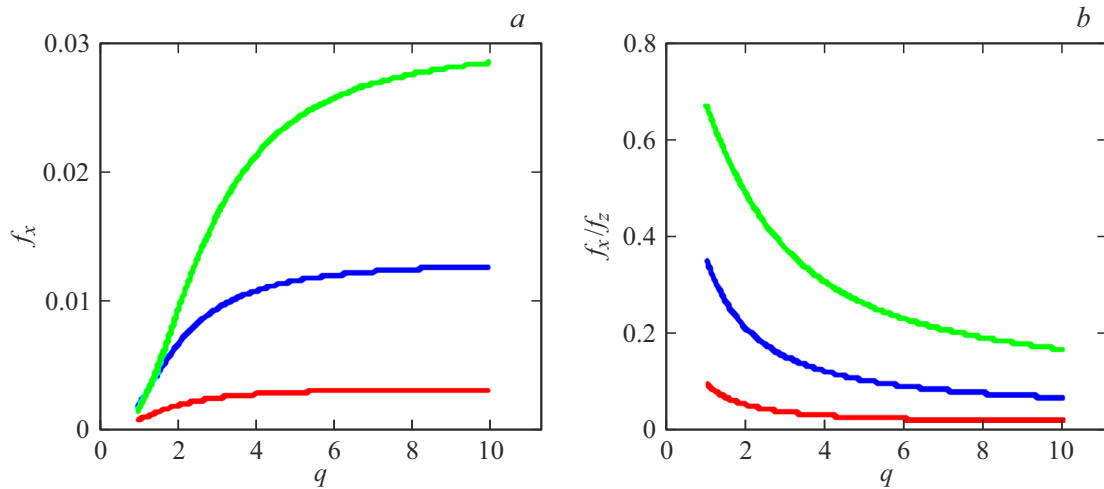


Figure 6. Dependence of friction force on reduced height $q = \sqrt{H/2R}$ of a parabolic probe (a) and ratio f_x/f_z of friction force to gravity force (b) at $z_0/R = 0.5$. Sequence of curves from top to bottom corresponds to parameters $a = 0.1, 0.5, 2$.

probe with the specified MFM cantilever shape we will get

$$Q = 0.98 \cdot 10^{-4} \left(\frac{h}{l} \right)^3 \frac{A}{R} \frac{w}{R} \left(\frac{\mu_s + 1}{\mu_s - 1} \right) \frac{E}{M_0^2} \frac{1}{\varphi_2(p, q, a_1)}, \quad (49)$$

$$\varphi_2(p, q, a_1) = \int_0^1 dy y (1 - y^2)^{-1/2} f_x(p, q, a_1 y), \quad (50)$$

where $a_1 = 4\pi A f \tau / (\mu_s + 1) R$, and $f_x(p, q, a_1) y = F_x / F_0$ — normalized friction force in (39), depending on parameters $a \equiv a_1 y, p, q$. For a spherical probe the numerical coefficient in (49) must be doubled, and instead of $\varphi_2(p, q, a_1)$ take a similar function produced when substituting in (50) the normalized friction force corresponding to (43). Value Q in (49) is now a function of $\tau / (\mu_s + 1)$ and has a more complex form.

Fig. 4 shows dependences of Q on τ for two types of probes at $\mu_s = 3, 10, 100$. Increased merit Q with growth of τ in these graphs is caused by reduced friction force (39) and (43) at $a \gg 1$ (fig. 2). Fig. 5 also provides dependences of Q on reduced distance $p = z_0/R$.

Dependences of friction and gravity forces on distance are monotonously decreasing. This follows from comparison of curves in fig. 2, 3, corresponding to different values p , and from fig. 5.

It is interesting to note that at small distances of probes from surface ($p = z_0/R = 0.1$) absolute values of gravity forces for a spherical probe are by an order less than for a parabolic one (with the same value R), and values of friction forces are close to each other (compare fig. 2 and 3). In addition, from fig. 2 it follows that for a spherical probe the friction forces may several times exceed the gravity forces in the field of dependence maximum $f_x(a)$. For a parabolic probe the reverse ratio is always true.

Fig. 6 provides dependences f_x and f_x/f_z on parameter $q = (H/2R)^{1/2}$, which characterizes length of a parabolic

probe. From fig. 6 it follows that at $q > 5$ increased length of the probe weakly influences force value f_x , but at the same time it is significantly decreased compared to gravity force f_z (fig. 6, b). Use of parabolic probes is probably more appropriate for sufficiently large distances of the probe from the surface ($z_0 \geq R$) due to slower decrease in forces of interaction with distance, which may be important when scanning surfaces with strongly developed topography. On the other hand, as it follows from fig. 4, 5, the merit behavior for probes of different types is different for different ratios of parameters τ and μ_s , so the choice of probe shape must be determined by the specific characteristics of the MP surface of the samples.

For magnetically coated probes, the magnitude of f_x and f_z forces is slightly reduced by module compared to probes made of homogeneous material. For example, for a solid vertically magnetized spherical probe with a radius of 20 nm and a probe with a radius of 15 nm having a magnetic shell with a thickness of 5 nm, located at a minimum distance of 10 nm from the surface, the difference in the gravity forces in the static case will be 16%.

The case of vertical motion of the probe with respect to the sample requires separate consideration, but in view of the close analogy with the case of electric dipole motion [14], we can expect that the numerical coefficients in the formulae for friction forces will be approximately two times higher.

Conclusion

Integral equations for the interaction force of a moving magnetized MFM probe with the surface of a nanostructured magnetic material with a general frequency dependence of magnetic permeability have been obtained. The cases of a small dipole particle and extended probes in the form of a paraboloid of rotation and a sphere have

been considered. Numerical calculations of the gravity and friction forces of the probe during nonrelativistic motion parallel to the surface for MP of relaxation type have been performed. The values of gravity and friction forces are of the same order, and in the case of a spherical probe the friction force can exceed the gravity force several times for some values of parameters.

Coefficients of merit of MFM oscillator in dynamic mode have been calculated. It is shown that merit dependence on the sample magnetic relaxation time has a characteristic minimum, the features of which depend on the probe shape and the value of the static MP of the sample. The results of the paper may be used for the development of a new method to study the frequency dispersion of magnetic permeability of materials using MFM.

Conflict of interest

The author declares that he has no conflict of interest.

Appendix

In accordance with the general method to solve differential equations of type (11), (12), it is necessary to find the sum of solutions to the corresponding homogeneous equations and partial solutions of inhomogeneous ones. In areas $z > 0$ and $z \leq 0$ the solution to a homogeneous equation $(d^2/dz^2 - k^2)y(z) = 0$ are functions $y(z) = C_1 \exp(-kz)$ and $y(z) = C_2 \exp(kz)$, where C_1 and C_2 — random constants. Partial solution of an inhomogeneous equation $(d^2/dz^2 - k^2)y(z) = f(z)$ (where $f(z)$ — known function) is found by fold $\int_{-\infty}^{+\infty} G(z, z') f(z') dz'$ of Green's function $G(z, z')$ with $f(z)$. Green's function $G(z, z')$ is a solution to equation

$$(d^2/dz^2 - k^2)G(z, z') = \delta(z - z') \quad (\text{A1})$$

in the field $-\infty < z < \infty$ and looks like

$$G(z, z') = -\frac{1}{2k} \exp(-k|z - z'|). \quad (\text{A2})$$

Partial solutions to equations (11), (12) are clearly found by simple multiplication (A2) by corresponding coefficients in the right-hand part of these equations. Given that, solution to equations (11) and (12) is written as

$$A_x = \begin{cases} A_1 \exp(-kz) + i \frac{(2\pi)^2}{k} k_y m_z \delta(\omega - k_x V) \\ \quad \times \exp(-k|z - z_0|), & z > 0, \\ B_1 \exp(kz), & z \leq 0, \end{cases} \quad (\text{A3})$$

$$A_y = \begin{cases} A_2 \exp(-kz) - i \frac{(2\pi)^2}{k} k_y m_z \delta(\omega - k_x V) \\ \quad \times \exp(-k|z - z_0|), & z > 0, \\ B_2 \exp(kz), & z \leq 0. \end{cases} \quad (\text{A4})$$

In equations (A3), (A4) indices \mathbf{k}, ω of Fourier components of vector potential A_x, A_y are omitted for simplicity. It should be noted that Fourier components of induced vector potential in the field $z > 0$ in (A3) and (A4) are matched with terms proportionate to A_1, A_2 . Since in the considered case $A_z = 0$, the condition of calibration $\text{div} \mathbf{A} = 0$ results in ratios $ik_x A_1 + ik_y A_2 = 0$ and $ik_x B_1 + ik_y B_2 = 0$, where

$$A_2 = -\frac{k_x}{k_y} A_1, \quad B_2 = -\frac{k_x}{k_y} B_1. \quad (\text{A5})$$

With account of link $\mathbf{H} = \text{rot} \mathbf{A}$ the conditions of continuity of intensity components H_x, H_y , and B_z in magnetic field induction at the boundary of $z = 0$ result in the requirement of continuity of values $\partial A_y / \partial z$, $\partial A_x / \partial z$ and $\mu(\partial A_y / \partial x - \partial A_x / \partial y)$. Taking into account these conditions and (A3)–(A5), we will get equations (13), (14) for Fourier components of induced vector potential. For coefficients B_1, B_2 in (A3) and (A4) we will accordingly have

$$B_1 = -A_1 + i \frac{(2\pi)^2}{k} k_y m_z \exp(-kz_0), \quad (\text{A6})$$

$$B_2 = A_1 \frac{k_x}{k_y} - i \frac{(2\pi)^2}{k} k_x m_z \exp(-kz_0), \quad (\text{A7})$$

but they are not required further, since to calculate force (1), only vector potential in the field $z > 0$ is used.

When calculating contributions to vector potential from components m_x, m_y of magnetic torque of the particle, we shall note that derivatives $\delta'(z - z')$, which are present in (7), (8), may be replaced for $k\delta(z - z')$, after that the equations for components of vector potential become fully analogous to equations (11), (12). As a result at $m_x \neq 0$, $m_y = m_z = 0$ and $A_{\mathbf{k}\omega, x} = 0$ for other Fourier components of vector potential we will get

$$A_{\mathbf{k}\omega, y}(z) = (2\pi)^2 m_x \left[\frac{\mu - 1}{\mu + 1} \exp(-k(z + z_0)) + \exp(-k|z - z_0|) \right] \delta(\omega - k_x V), \quad (\text{A8})$$

$$A_{\mathbf{k}\omega, z}(z) = i \frac{(2\pi)^2}{k} k_y m_x \left[\frac{\mu - 1}{\mu + 1} \exp(-k(z + z_0)) - \exp(-k|z - z_0|) \right] \delta(\omega - k_x V). \quad (\text{A9})$$

In case of $m_y \neq 0$, $m_x = m_z = 0$ and $A_{\mathbf{k}\omega, y} = 0$ accordingly we will have

$$A_{\mathbf{k}\omega, x}(z) = -(2\pi)^2 m_y \left[\frac{\mu - 1}{\mu + 1} \exp(-k(z + z_0)) + \exp(-k|z - z_0|) \right] \delta(\omega - k_x V), \quad (\text{A10})$$

$$A_{\mathbf{k}\omega, z}(z) = -i \frac{(2\pi)^2}{k} k_y m_x \left[\frac{\mu - 1}{\mu + 1} \exp(-k(z + z_0)) - \exp(-k|z - z_0|) \right] \delta(\omega - k_x V). \quad (\text{A11})$$

References

- [1] A.N. Lagarkov, K.N. Rozanov. *J. Magn. Magn. Mater.*, **321**, 2082 (2009). DOI: 10.1016/j.jmmm.2008.08.099
- [2] X.G. Chen, Y. Ye, J.P. Cheng, *J. Inorg. Mater.*, **26**, 449 (2011). DOI: 10.3724/sp.j.1077.2011.00449
- [3] F.M. Idris, M. Hashim, Z. Abbas, I. Ismail, R. Nazlan, I.R. Ibrahim. *J. Magn. Magn. Mater.*, **405**, 197 (2016). DOI: 10.1016/JJMMM.2015.12.070
- [4] Zirui Jia, Di Lan, Kejun Lin, Ming Qin, Kaichang Kou, Guanglei Wu, Hongjing Wu, *J. Mat. Sci.: Mater. Electron.*, **29**, 17122 (2018). <https://doi.org/10.1007/s10854-018-9909-z>
- [5] S.Y. Bobrovskii, V.A. Garanov, A.S. Naboko, A.V. Osipov, K.N. Rozanov, *EPJ Web of Conf.* **185**, 02002 (2018). <https://doi.org/10.1051/epjconf/201818502002>
- [6] S.S. Maklakov, A.N. Lagarkov, S.A. Maklakov, Y.A. Adamovich, D.A. Petrov, K.N. Rozanov, I.A. Ryzhikov, A.Y. Zarubina, K.V. Pokholok, D.S. Filimonov. *J. Alloys Compoun.*, **706**, 267 (2017). <https://doi.org/10.1051/epjconf/201818502002>
- [7] T. Nakamura, T. Tsutaoka, K. Hatakeyama. *J. Magn. Magn. Mater.*, **138**, 319 (1994). DOI: 10.1016/0304-8853(94)90054-X
- [8] K.A. Rozanov. Avtoref. dis. doktora fiz.-mat. nauk (Institut teoreticheskii i prikladnoy elektrodinamiki RAN, M., 2018) (in Russian), <https://istina.msu.ru/dissertations/106198705>
- [9] J.A. Sidles, J.L. Garbini, K.J. Bruland, D. Rugar, O. Zuger, S. Hoen, C.S. Yannoni. *Rev. Mod. Phys.*, **67**, 249 (1995). <https://doi.org/10.1103/RevModPhys.67.249>
- [10] M.R. Koblischka, U. Hartmann. *Ultramicroscopy*, **97**, 103 (2003). DOI: 10.1109/TMAG.2009.2021985
- [11] D. Rugar, R. Budakian, H.J. Mamin. *Nature*, **403**, 329 (2004). DOI: 10.1038/nature02658
- [12] C.L. Degen, M. Poggio, H.J. Mamin, C.T. Rettner, D. Rugar, *Proc. Nat. Acad. Sci. USA*, **106**, 1313 (2009). DOI: 10.1073/pnas.0812068106
- [13] J.D. Jackson, *Classical Electrodynamics* (J. Wiley & Sons, NY.–London, 1962)
- [14] G.V. Dedkov, A.A. Kyasov. *Phys. Low-Dim. Struct.*, **1/2**, 1 (2003).
- [15] I.S. Gradshteyn, I.M. Ryzhik. *Tables of Integrals, Series and Products* (Acad. NY., 2000)
- [16] D.A. Vinnik, V.E. Zhivulin, D.P. Sherstyuk, A.Yu. Starikov, P.A. Zezyulina, S.A. Gudkova, D.A. Zherebtsov, K.N. Rozanov, S.V. Trukhanov, K.A. Astapovich, S.B. Sombra, D. Zhou, R.B. Jotania, C. Singh, A.V. Trukhanov. *J. Mater. Sci. C*, **9**, 5425 (2021). DOI: 10.1039/d0tc05692h
- [17] Ch. Kittel. *Introduction to Solid State Physics* (Wiley, 1996)